Low-lying electronic states and molecular structure of Fe_2O_2

Zexing Cao,[a] **Miquel Duran**[b] **and Miquel Solà**[*b]

[a] *Department of Chemistry and Institute of Physical Chemistry, Xiamen University, Xiamen 361005, People's Republic of China*
[b] *Institute of Computational Chemistry and Department of Chemistry, Universitat de Girona, 17071 Girona, Catalonia, Spain. E-mail: miquel@iqc.udg.es*

The structure, bonding and relative stabilities of the ground and low-lying excited states of Fe_2O_2 have been studied by the hybrid B3LYP density-functional and coupled-cluster molecular orbital methods. Calculations indicate that the $(\mu\text{-}O)_2$ rhombic $^7B_{2u}$ state is the ground state for Fe_2O_2. Stable molecular diiron oxo $Fe_2\text{-}O_2$ complexes in distorted tetrahedral and planar side-on modes have been also located on the potential-energy hypersurfaces of Fe_2O_2. The calculated IR-active frequencies corresponding to two in-plane deformations of the rhombic ring agree well with the observed values. The bonding features of the $(\mu\text{-}O)_2$ rhombic Fe_2O_2 have been discussed based on natural bond orbital and Bader topological analyses. These analyses show that an effective Fe—Fe bonding across the ring exists in the $^7B_{2u}$ ground state.

Introduction

The interaction of iron with molecular oxygen has achieved a considerable interest in current experimental and theoretical studies because it is involved in a wide range of processes, from corrosion of materials to oxygen transportation in biological systems. Many studies have been devoted to monoiron oxides. Among them, the diatomic FeO molecule has been the most thoroughly investigated.[1–9] Experimental and theoretical investigations of the triatomic FeO_2, FeO_2^- and FeO_2^+ have been also carried out.[1,10–18] The higher monoiron oxides FeO_4 and FeO_4^- have been observed experimentally,[18,19] and their structures and molecular bonding have been studied theoretically.[20] However, to date, only a few studies have been performed on the structure and bonding of diiron oxides.

Diiron oxo complexes are a common structural motif in a class of metalloproteins that are important as oxygen carriers.[21,22] In a recent study,[23] it has been demonstrated that a high-valent Fe_2O_2 diamond core can constitute the common structural unit for high-valent intermediates in the oxygen activation mechanisms of non-heme iron enzymes.[24] A high-valent non-heme diiron intermediate and the first bis(μ-oxo) diiron(III) complex have been recently synthesized.[2,26] Further, extended X-ray absorption fine structure (EXAFS) and Mössbauer spectroscopy studies have provided direct experimental evidence for the participation of a $(\mu\text{-}O)_2$ rhombic Fe_2O_2 diamond core (structure I in Fig. 1) in the catalytic cycle of methane monoxygenase.[27] On the other hand, a recent anion photoelectron spectroscopy study has suggested the existence of $(\mu\text{-}O)_2$ rhombic Fe_2O_2 and possible isomers containing an unbroken O—O bond.[19] IR spectra, complemented with density functional calculations of several electronic states of different iron oxide product molecules in the reactions of laser-ablated iron atoms with molecular oxygen, have indicated that the $(\mu\text{-}O)_2$ rhombic Fe_2O_2 absorbs at 517.4 and 660.6 cm^{-1}.[18] Finally, Fe_2O_2 species have also been produced through reaction of free iron clusters with molecular oxygen.[28]

Despite all these important contributions, the question of how many Fe_2O_2 isomers exist and which are the most stable remains still open. In this work, we have carried out a theoretical investigation on Fe_2O_2 with the B3LYP hybrid DFT functional and *ab initio* molecular methods. Eight possible structures have been analyzed in our calculations (Fig. 1).

Computational details

Density functional theory (DFT) calculations have been performed with the Becke's three-parameters hybrid exchange functional[29] and the non-local correlation functional of Lee, Yang and Parr[30] (B3LYP) to obtain the optimized geometries, energies, vibrational frequencies and corresponding intensities
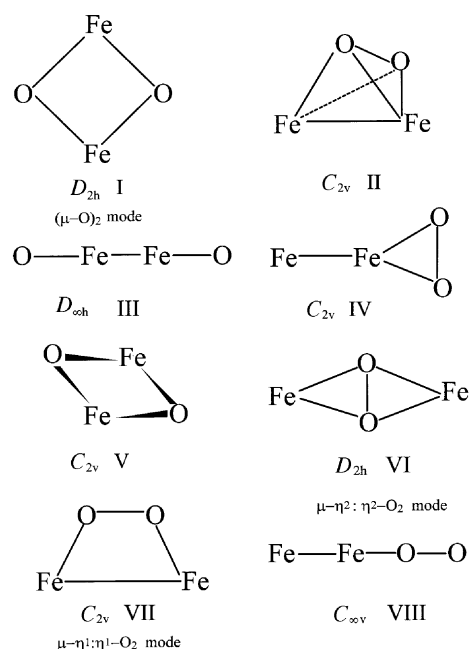

Fig. 1 The eight possible structures for Fe_2O_2 considered in this study.

of the ground and low-lying excited states of Fe_2O_2. The computational efficiency and accuracy of the B3LYP method have been very well documented for transition metal complexes.[31–34] In particular, previous studies on FeO_2 [10.18] showed that the hybrid B3LYP approach works reasonably well. Single and double substitutions with non-iterative triple excitations coupled cluster [CCSD(T)][35,36] energy calculations for several selected states have been carried out at the optimized B3LYP geometries (CCSD(T)//B3LYP) to confirm the validity of this approach.

The initial guesses of electron configurations for the low-lying states of Fe_2O_2 are obtained by altering molecular orbitals from converged SCF calculations at different geometries. All calculations have been done within the unrestricted methodology, except for singlets, which have been calculated within the restricted formalism. The basis set used for all atoms has been the 6-311G*,[37,38] which, for iron, is the all-electron basis set of Wachters and Hay[39,40] with the scaling factors of Raghavachari and Trucks.[41] The polarization functions for iron and oxygen atoms are an f function with an exponent of 1.05 and a d function with an exponent of 1.292, respectively. All calculations have been performed with Gaussian 94,[42] except for Bader topological analyses that were carried out by means of the Electra program.[43]

Results and discussion

The electron configurations, optimized geometries, harmonic vibrational frequencies and relative energies for some selected low-lying states of the $(\mu\text{-O})_2$ rhombic, distorted tetrahedral, and side-on Fe_2O_2 are presented in Table 1. Only the most stable states obtained for each multiplicity are included. Information about other states can be found in the supplementary material†

---

† Supplementary material (**SUP** 57424, 9 pp.) deposited with the British Library. Details are available from the Editorial Office.

Energetics

The results in Table 1 show that the ground state of Fe_2O_2 is the $^7B_{2u}$ state of the $(\mu\text{-O})_2$ rhombic structure D_{2h} I. At the CCSD(T)//B3LYP level, the ^5A_g, $^3B_{1u}$ and the ^1A_g states of the rhombic structure are higher in energy than the lowest $^7B_{2u}$ state by 117, 150 and 160 kJ mol^{-1}, respectively. The energy ordering predicted by the B3LYP method is in agreement with the CCSD(T)//B3LYP calculation for these states, although the larger energy differences between the low-spin and high-spin states indicate that the B3LYP method tends to overestimate the stability of the latter. The higher stability of the state with high spin was also found for Fe_2 [44] and for rhombic $(CoO)_2$.[45] All attempts to find a distorted $(\mu\text{-O})_2$ rhombic state $^3A_2$, which was the most stable among the several states considered in a previous study,[45] have failed. It is noteworthy that the same authors[45] indicated that this state was probably an artifact of their calculation. Furthermore, the single-point calculation of the $^3A_2$ state at the geometry reported[45] has been found to be higher in energy than other triplet states of the $(\mu\text{-O})_2$ rhombic structure. In addition to the most stable $(\mu\text{-O})_2$ rhombic isomer, much less stable states corresponding to C_{2v} II and C_{2v} VII structures were located. These can be considered as molecular diiron oxo Fe_2—O_2 complexes and they might account for the low electron affinity isomers detected in a previous photoelectron spectroscopy experiment.[19]

Very few stable states with the other possible structures depicted in Fig. 1 were found in the present study. The singlet state $^1A_1$ in C_{2v} IV structure has a large Fe—Fe separation of 3.107 Å and can be considered a van der Waals complex between Fe and FeO_2. Similar behaviour has been found for the states of higher spin in the C_{2v} IV structure. This implies that the interaction of the d orbitals of Fe and the bonding $1\pi_u$ and antibonding $1\pi_g$ of O_2 is strong and breaks the Fe—Fe bond. No stable complexes with C_{2v} V structure have been found. During the optimization of the states of lower spin for the $(\mu\text{-}\eta^2\!:\eta^2\text{-}O_2)$ D_{2h} VI isomer the O—O bond is

Table 1 Electronic configurations, geometries, energies and vibrational frequencies obtained with the B3LYP method for some selected low-lying states of Fe_2O_2

State	Configuration[a]	Geometry[b]	ΔE[c]	ZPE[d]	Frequencies[e]
D_{2h}I					
^1A_g	$4a_g^2 2b_{2u}^2 3b_{1u}^2 b_{3g}^2 b_{2g}^2 b_{1g}^2 a_u^2 b_{2g}^2$	2.476, 1.714, 2.372	423.9(159.9)	21.8	285(74), 379(0), 629(2), 725(126), 801(0), 758(0)
$^3B_{1u}$	$4a_g^2 2b_{2u}^2 3b_{1u}^2 b_{3g}^2 b_{1g}^2 b_{3u}^2 a_u^2 b_{2g}^2 b_{3u}$	2.364, 1.731, 2.530	231.4(149.8)	19.5	279(72), 353(0), 523(9), 617(0), 692(223), 804(0)
^5A_g	$4a_g^2 2b_{2u}^2 3b_{1u}^2 b_{3g}^2 b_{1g}^2 b_{3u} a_u b_{2g} b_{1g}$	2.447, 1.770, 2.558	79.5(116.9)	18.4	180(94), 321(0), 563(0), 574(218), 686(142), 750(0)
$^7B_{2u}$	$4a_g^2 2b_{2u}^2 2b_{1u}^2 b_{3u} b_{3g} b_{3g} b_{1g} a_u b_{2g} b_{3g}$ $b_{1u} b_{1g} b_{3u}$	2.203, 1.790, 2.821	0.0(0.0)	19.2	203(94), 401(0), 484(0), 657(87), 737(0), 738(109)
C_{2v}II					
$^1A_1$	$6a_1^2 3b_2^2 3b_1^2 2a_2^2$	1.885, 1.466, 76.7	702.6	17.7	245(0), 340(0), 437(16), 503(9), 568(32), 874(43)
$^5A_1$	$6a_1^3 3b_2^2 2b_1^2 a_2^2 2b_1 2a_2$	1.551, 2.377, 73.6	564.1	16.2	220(8), 338(257), 395(0), 489(33), 500(0), 767(30)
C_{2v}VII					
$^1A_1$	$6a_1^2 3b_2^2 3b_1^2 2a_2^2$	1.913, 1.437, 82.2	751.1	18.5	230(0), 297(20), 423(7), 640(2), 686(22), 816(105)
$^3B_1$	$6a_1^2 3b_2^2 3b_1 a_2^2 a_2 b_2$	1.942, 1.424, 81.5	665.3	20.3	345(0), 375(6), 492(0), 656(2), 728(4), 804(158)
$^5A_2$	$6a_1^2 2b_2^2 3b_1 a_2^2 a_2 2b_2 a_1$	1.847, 1.303, 82.2	585.3	17.5	209(16), 254(0), 324(9), 427(12), 502(3), 1213(131)
$^7A_1$	$6a_1^2 2b_2^2 2b_1 a_2^2 a_2 3b_2 b_1 a_1$	2.011, 1.317, 80.5	448.9	15.9	162(6), 181(0), 329(26), 373(9), 418(0), 1194(90)
Fe_2					
$^5\Delta_u$	$2\sigma_g^2 \pi_u^4 \delta_g^3 \delta_u^2 \pi_g^2 \sigma_u^\beta$	1.876	75.4	2.9	483(0)
$^7\Delta_u$	$2\sigma_g^2 \pi_u^4 \delta_g^3 \delta_u^2 \pi_g^2 \sigma_u^1$	1.906	0.0	2.8	469(0)
FeO					
$^3\Sigma$	$2\sigma^2 \pi_u^4 \delta_u^2 \pi^2$	1.614	207.1	5.7	951(70)
$^5\Delta$	$\sigma^2 \pi^4 \delta^3 \pi^2 \sigma^1$	1.606	0.0	5.4	906(97)
O_2					
$^1\Delta_g$	$2\sigma_g^2 \sigma_u^2 \pi_u^4 \pi_g^2$	1.207	163.3	9.7	1626(0)
$^3\Sigma_g^-$	$2\sigma_g^2 \sigma_u^2 \pi_u^4 \pi_g^2$	1.206	0.0	9.8	1641(0)

[a] Core electrons are omitted, and numbers in front of molecular orbitals indicate the number of orbitals with the same symmetry in the wavefunction. [b] The bond lengths in Å, and bond angles in degrees. D_{2h} I: Fe—Fe, Fe—O, O—O, respectively; C_{2v} II: Fe—O, O—O, Fe—O—Fe, respectively; C_{2v} VII: Fe—Fe, O—O, O—Fe—Fe, respectively. [c] B3LYP relative energies, in kJ mol^{-1}, referred to the computed ground state for each species. Values in parentheses have been computed at the CCSD(T)//B3LYP level. B3LYP total energies for the ground states are -2677.796514 au (-2675.154177 au at the CCSD(T)//B3LYP level) for the $^7B_{2u}$ state of Fe_2O_2, -2527.1684490 au for the $^7\Delta_u$ state of Fe_2, -1338.827379 au for the $^5\Delta$ state of FeO, and -150.364786 au for the $^3\Sigma_g^-$ state of O_2. [d] Zero-point vibrational energies, computed at the B3LYP level, given in kJ mol^{-1}. [e] Frequencies in cm^{-1}; intensities, in parentheses, in km mol^{-1}.

broken, thus yielding the (μ-O)$_2$ rhombic D_{2h} I species. The low stability of Fe$_2$O$_2$ complexes with the (μ-η^2: η^2-O$_2$) rhombic structure VI is in accordance with the fact that no Fe$_2$O$_2$ complex with this structure has been synthesized yet.[46] The states of high spin for the linear $D_{\infty h}$ III structure are not stable. The same has been found for the linear Fe—Fe—O—O (structure VIII in Fig. 1), and the states of high spin in $C_{\infty v}$ symmetry dissociate to Fe + FeOO. Calculated results for these less stable isomers and higher-order saddle points are not presented here.

Note that the results obtained for the diiron oxo Fe$_2$—O$_2$ complexes are different from those reported for the Fe$_2$—N$_2$ species.[47] Among the Fe$_2$—N$_2$ species, the linear Fe—Fe—N—N septet state was found to be the most stable, and stable states of lower spin in linear symmetry were also located. The difference in the most stable molecular structure between Fe$_2$—O$_2$ and Fe$_2$—N$_2$ can be attributed to the different highest occupied molecular orbitals (HOMO) of N$_2$ and O$_2$. The HOMO of N$_2$ is a 3σ_g orbital, while the HOMOs of O$_2$ are singly occupied (for the triplet) and doubly occupied (for the singlet) 1π_g orbitals. The linear end-on mode is thus favoured in Fe$_2$—N$_2$, through interaction between the lowest unoccupied molecular orbital (LUMO) 7σ_u and singly occupied HOMO 6σ_u of Fe$_2$ in its ground state and the 3σ_g of N$_2$. For O$_2$ the same 3σ_g orbital is much lower in energy and, therefore, less suitable for the linear interaction than the 3σ_g of N$_2$. The Fe$_2$—O$_2$ complexes prefer the side-on and tetrahedral modes through the interaction between singly occupied lower in energy 1δ_g and 3π_g orbitals of Fe$_2$ and the HOMO 1π_g of O$_2$. Comparison between the results obtained for Fe$_2$—O$_2$ and Fe$_2$—N$_2$ species shows that the interaction of Fe$_2$ with O$_2$ is stronger than that of Fe$_2$ and N$_2$.

Table 2 lists the dissociation energies computed at the B3LYP level corresponding to different dissociation products for some selected states of the rhombic, tetrahedral and side-on structures. The states of the rhombic isomer in Table 2 are lower in energy than the products of the six dissociation channels considered here, except for the ^{1}A$_g$ state relative to the ground state of FeO. Dissociation of the (μ-O)$_2$ rhombic ^{7}B$_{2u}$ state to two $^5\Delta$ FeO is endothermic by 364 kJ mol^{-1}. This value can be compared with the 301 kJ mol^{-1} for the dissociation of the ^{7}A$_u$ (CoO)$_2$ system to 2CoO molecules.[45] The tetrahedral and side-on diiron oxo Fe$_2$—O$_2$ complexes are more stable than the products Fe$_2$ + O$_2$, except for the singlet states relative to the ground states Fe$_2$($^7\Delta_u$) + O$_2$($^3\Sigma_g^-$). Considering the spin multiplicity of the initial and final states, the dissociation of the singlet states of Fe$_2$—O$_2$ into the septet Fe$_2$ and the triplet O$_2$ is not likely, and the singlet molecular
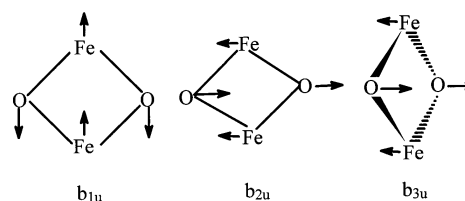

Fig. 2 The three IR-active vibrational modes for rhombic (μ-O)$_2$ Fe$_2$O$_2$.

diiron oxo Fe$_2$—O$_2$ complexes should be correlated to certain excited states of Fe$_2$ with lower spin.

Vibrational frequencies

For the (μ-O)$_2$ rhombic isomer, there are only three IR-active vibrational modes corresponding to two deformations in plane and one out of plane, which are depicted in Fig. 2 The 517.4 and 660.6 cm^{-1} frequencies with 16/18 isotopic ratios of 1.0457 and 1.0454, respectively, observed in reactions of laser-ablated iron atoms with oxygen molecules have been assigned to Fe$_2$O$_2$ species.[10,18,45] The B3LYP calculated frequencies in Table 1 agree with these observed values for certain stable states of the (μ-O)$_2$ rhombic structure. For the ^{3}B$_{1u}$ state, the strong band at 692(223) cm^{-1} is also in reasonable agreement with the observed 660.6 cm^{-1}. Further, its calculated harmonic 16/18 isotopic ratio of 1.0453 agrees with the observed 1.0454. The lower ^{5}A$_g$ quintet state has strong absorptions at 574(218) and 686(142) cm^{-1}, which are only slightly higher than the observed values. The ^{5}A$_g$ state has calculated 16/18 isotopic ratios of 1.0475 for the 574(218) cm^{-1} and 1.0457 for the 686(142) cm^{-1}, to be compared to the observed 1.0457 and 1.0454, respectively. Finally, the ground-state ^{7}B$_{2u}$ has a band at 657(87) cm^{-1} and a corresponding 16/18 isotopic ratio of 1.0462. Unfortunately, states of different symmetry and spin multiplicity can account for the observed values and, therefore, a definite assignment is not possible. However, it is worth noting that all vibrational modes with frequencies close to the observed bands at 517.4 and 660.6 cm^{-1} are in plane b$_{1u}$ and b$_{2u}$ deformations of the rhombic ring.

Bonding features

We have carried out a natural population and natural bond orbital (NBO) analysis in order to get a further insight into the bonding features of the (μ-O)$_2$ rhombic Fe$_2$O$_2$. Tables 3 and 4 present the results of this natural population and NBO analysis. Note that the natural charges, as well as the Mulliken charges in Table 3, increase as the spin multiplicity

Table 2 Dissociation energies^a corresponding to different dissociation limits for the lower stable states in the rhombic, tetrahedral and side-on isomers computed at the B3LYP level

| State | Dissociation limits | | | | | |
	2FeO($^5\Delta$)	2FeO($^3\Sigma$)	Fe$_2$($^7\Delta_u$) + O$_2$($^3\Sigma_g^-$)	Fe$_2$($^7\Delta_u$) + O$_2$($^1\Delta_g$)	Fe$_2$($^5\Delta_u$) + O$_2$($^3\Sigma_g^-$)	Fe$_2$($^5\Delta_u$) + O$_2$($^1\Delta_g$)
D_{2h} I						
^{1}A$_g$	−62.8	351.9	258.1	1226.7	333.5	496.6
^{3}B$_{1u}$	136.4	546.4	452.7	615.9	528.4	691.6
^{5}A$_g$	284.9	699.6	606.3	769.4	681.2	844.3
^{7}B$_{2u}$	363.6	777.8	684.1	847.3	759.4	922.6
C_{2v} II						
^{1}A$_1$	−337.2	77.4	−16.7	146.4	59.0	222.2
^{5}A$_1$	−197.1	217.1	123.4	286.6	198.7	361.9
C_{2v} VII						
^{1}A$_1$	−386.2	28.0	−65.7	97.5	9.6	172.8
^{3}B$_1$	−302.5	112.1	18.0	181.2	93.7	256.9
^{5}A$_2$	−219.7	194.6	100.8	264.0	176.6	339.7
^{7}A$_1$	−81.6	332.6	209.6	372.8	314.2	477.4

^{a} The dissociation energies are defined by the difference: E (dissociation limits) $- E$ (Fe$_2$O$_2$), in kJ mol^{-1}. Zero-point vibrational energies have been included in the calculation.

Table 3 Natural population analysis of the lower states of the rhombic Fe_2O_2 at the B3LYP level, showing natural charge q (with corrsponding Mulliken charges in parentheses) and effective valence-shell natural electron configuration (NEC)

State	Atom	q^a	NEC
^1A_g	Fe	0.729(0.690)	$4s^{0.68}3d^{6.59}$
	O	−0.729(−0.690)	$2s^{1.90}2p^{4.82}$
$^3B_{1u}$	Fe	0.811(0.745)	$4s^{0.67}3d^{6.51}$
	O	−0.811(−0.745)	$2s^{1.91}2p^{4.89}$
^5A_g	Fe	0.919(0.825)	$4s^{0.66}3d^{6.41}$
	O	−0.919(−0.825)	$2s^{1.92}2p^{4.99}$
$^7B_{2u}$	Fe	0.972(0.860)	$4s^{0.61}3d^{6.40}$
	O	−0.972(−0.860)	$2s^{1.90}2p^{4.82}$

^{a} In atomic units (electron charge).

Table 5 Bader analysis for the lower states of the $(\mu\text{-O})_2$ rhombic Fe_2O_2 species computed at the B3LYP level

State	Critical point	$r_c{}^a$	$\rho(r_c)^b$	$\nabla^2\rho(r_c)^b$	$|\lambda_1|/\lambda_3$
^1A_g	(3, 1)	1.238	0.061	0.272	0.385
	Fe—O(3, −1)	0.850	0.180	0.849	0.187
$^3B_{1u}$	(3, 1)	1.182	0.069	0.241	0.329
	Fe—O(3, −1)	0.868	0.179	0.739	0.236
^5A_g	(3, 1)	1.223	0.060	0.205	0.351
	Fe—O(3, −1)	0.891	0.166	0.592	0.267
$^7B_{2u}$	Fe—Fe(3, −1)	1.102	0.097	0.187	0.343
	Fe—O(3, −1)	0.912	0.162	0.572	0.258

^{a} Distance from the critical point to the closest Fe atom in Å. ^{b} In atomic units (e a_0^{-3} and e a_0^{-5}).

increases, showing that more electronic charge is transferred from Fe to O, and implying that the bonding interaction becomes stronger with the increase in spin multiplicity. This is consistent with the relative stabilities predicted by the B3LYP and CCDS(T)//B3LYP methods. Results of the Bader analysis[48] collected in Table 5, indicate that the Fe—O bond has ionic character, as can be deduced from the small density, positive laplacian, and small ratio between the perpendicular and the parallel curvatures at the bond critical point ($|\lambda_1|\,\lambda_3$).

It is interesting to discuss whether an Fe—Fe bond exists in the $(\mu\text{-O})_2$ rhombic Fe_2O_2. From the NBO results in Table 4 one can see that an effective Fe—Fe antibonding interaction exists for the ^1A_g and $^3B_{1u}$ states, while an effective bonding for the Fe—Fe bond is present in the lowest $^7B_{2u}$ state. Finally, no Fe—Fe bonding across the ring is observed for the

^5A_g state. This is in agreement with the results of Table 5, which show that a bond critical point between Fe—Fe exists only for the most stable $^7B_{2u}$ state. Surprisingly, there are NBOs for the alpha electrons between the two O atoms in the lowest septet state, despite the large O—O separation of 2.821 Å and the fact that no bond critical point has been found connecting the two oxygen atoms. This suggests a strong electron delocalization in this state.

Conclusions

We have investigated the low-lying states of Fe_2O_2 with the B3LYP and CCSD(T) methodologies. The molecular structure and harmonic vibrational frequencies for these states have been reported. The $^7B_{2u}$ $(\mu\text{-O})_2$ rhombic state has been found to be the ground state for Fe_2O_2. The existence of an effective Fe—Fe bonding for this state is confirmed by the NBO and Bader analyses. At the CCSD(T) level, the ^5A_g, $^3B_{1u}$ and ^1A_g states are less stable than the $^7B_{2u}$ state by 117, 150 and 160 kJ mol^{-1}, respectively. Interestingly, the energy ordering for the lower states of the $(\mu\text{-O})_2$ rhombic Fe_2—O_2 structure given by the B3LYP approach is in agreement with the CCSD(T) calculations, although the energy differences between low-spin and high-spin states are overestimated by the B3LYP approach. The observed IR bands at 660.6 and 514.7 cm^{-1} have been assigned to two in-plane deformation modes of the rhombic ring. Finally, the distorted tetrahedral and planar side-on modes are the most stable structures for the diiron oxo Fe_2—O_2 complexes.

Table 4 Principal NBOs for the lower states of the $(\mu\text{-O})_2$ rhombic Fe_2O_2 species calculated at the B3LYP level, with orbital energies, occupancies and compositions $(c_A h_A + c_B h_B)$ in terms of hybrids (h) on A and B with c_A and c_B being the corresponding expansion coefficients (A,B = Fe,O)

NBO^a A—B	Energy^b	Occupancy	c_A	h_A	c_B	h_B
^1A_g						
Fe—Fe*(2)	−0.1518	1.9999	0.7071	d	−0.7071	d
Fe—O(4)	−0.5004	1.9862	0.4463	$sd^{1.5}$	0.8949	$sp^{7.9}$
Fe—Fe	−0.1384	0.4279	0.7071	d	0.7071	d
Fe—Fe	−0.1289	0.7624	0.7071	d	0.7071	d
$^3B_{1u}$						
Alpha electrons						
Fe—Fe*	−0.1982	0.9999	0.7071	d	−0.7071	d
Fe—O(4)	−0.4763	0.9907	0.4686	$sd^{1.33}$	0.8834	$sp^{11.39}$
Fe—Fe	−0.1635	0.2879	0.7071	d	0.7071	d
Beta electrons						
Fe—Fe*	−0.1687	0.9998	0.7071	d	−0.7071	d
Fe—O(4)	−0.4918	0.9935	0.4423	$sd^{1.62}$	0.8969	$sp^{9.15}$
Fe—Fe	−0.1330	0.2523	0.7071	d	0.7071	d
^5A_g						
Alpha electrons						
Fe—O(4)	−0.4236	0.9863	0.5117	$sd^{1.25}$	0.8591	$sp^{17.4}$
Beta electrons						
Fe—O(4)	−0.4539	0.9946	0.4449	$sd^{1.5}$	0.8956	sp^9
Fe—O(2)	−0.2602	0.9317	0.2703	d	0.9628	p
$^7B_{2u}$						
Alpha electrons						
Fe—Fe*	−0.2708	0.9972	0.7071	d	−0.7071	d
Fe—Fe	−0.2749	0.5943	0.7071	d	0.7071	d
O—O	−0.3444	0.8512	0.7071	$sp^{38.77}$	0.7071	$sp^{38.77}$
O—O*	−0.2432	0.4102	0.7071	$sp^{38.77}$	−0.7071	$sp^{38.77}$
Beta electrons						
Fe—Fe	−0.2081	0.8820	0.7071	$sd^{3.04}$	0.7071	$sd^{3.04}$
Fe—O(4)	−0.4417	0.9895	0.4298	$sd^{2.49}$	0.9029	$sp^{11.28}$
Fe—O(2)	−0.2575	0.9269	0.2805	d	0.9599	p

^{a} The numbers in parentheses indicate the number of equivalent NBOs. ^{b} In atomic units.

References

1 J. Fan and L. S. Wang, *J. Chem. Phys.*, 1995, **102**, 8714.
2 A. J. Merer, *Annu. Rev. Phys. Chem.*, 1989, **40**, 407.
3 M. Dolg, U. Wedig, H. Stoll and H. Preuss, *J. Chem. Phys.*, 1987, **86**, 2123.
4 T. C. Steimle, D. F. Nachman and J. E. Shirley, *J. Chem. Phys.*, 1989, **90**, 5360.
5 T. Andersen, K. R. Lykke, D. M. Neumark and W. C. Lineberger, *J. Chem. Phys.*, 1987, **6**, 1858.
6 T. Kroeckertskothen, H. Knockel and E. Tiemann, *Chem. Phys.*, 1986, **103**, 335; *Mol. Phys.*, 1987, **62**, 1031.
7 A. W. Taylor, A. S.-C. Cheung and A. J. Merer, *J. Mol. Spectrosc.*, 1985, **113**, 487.
8 D. W. Green and G. T. Reedy, *J. Mol. Spectrosc.*, 1979, **78**, 257 and references therein.
9 P. C. Engelking and W. C. Lineberger, *J. Chem. Phys.*, 1977, **62**, 2566.
10 L. Andrews, G. V. Chertihin, A. Ricca and C. W. Bauschlicher, *J. Am. Chem. Soc.*, 1996, **118**, 467.
11 Z. Cao, M. Duran and M. Solà, *Chem. Phys. Lett.*, 1997, **274**, 411.

12 D. Schröder, A. Fiedler, J. Schwarz and H. Schwarz, *Inorg. Chem.*, 1994, **33**, 5094.

13 M. Fanfarillo, H. E. Cribb, A. J. Downs, T. M. Greene and M. J. Almond, *Inorg. Chem.*, 1992, **31**, 2962.

14 P. D. Lyne, D. M. P. Mingos, T. Ziegler and A. J. Downs, *Inorg. Chem.*, 1993, **32**, 4785.

15 S. A. Mitchell and P. A. Hackett, *J. Chem. Phys.*, 1990, **93**, 7822.

16 S. Abramowitz, N. Acquista and I. W. Levin, *Chem. Phys. Lett.*, 1977, **50**, 423.

17 (a) S. Chang, G. Blyholder and J. Fernandez, *Inorg. Chem.*, 1981, **20**, 2813; (b) G. Blyholder, J. Head and F. Ruette, *Inorg. Chem.*, 1982, **21**, 1539; (c) M. Helmer and J. M. C. Plane, *J. Chem. Soc., Faraday Trans.*, 1994, **90**, 395.

18 G. V. Chertihin, W. Saffel, J. T. Yustein, L. Andrews, M. Neurock, A. Ricca and C. W. Bauschlicher, *J. Phys. Chem.*, 1996, **100**, 5261.

19 H. Wu, S. R. Desai and L. S. Wang, *J. Am. Chem. Soc.*, 1996, **118**, 5296.

20 Z. Cao, W. Wu and Q. Zhang, submitted for publication.

21 B. P. Murch, P. D. Boyle and L. Que, Jr., *J. Am. Chem. Soc.*, 1985, **107**, 6728.

22 A. C. Rosenzweig and S. Lippard, *Acc. Chem. Res.*, 1994, **27**, 229.

23 C. Kim, Y. Dong and L. Que, Jr., *J. Am. Chem. Soc.*, 1997, **119**, 3635.

24 L. Que, Jr. and Y. Dong, *Acc. Chem. Res.*, 1996, **29**, 190.

25 Y. Dong, H. Fujii, M. P. Hendrich, R. A. Leising, G. Pan, C. R. Randall, E. C. Wilkinson, Y. Zang, L. Que, Jr., B. G. Fox, K. Kauffmann and E. Münck, *J. Am. Chem. Soc.*, 1995, **117**, 2778.

26 (a) Y. Zang, Y. Dong, L. Que, Jr., K. Kauffmann and E. Münch, *J. Am. Chem. Soc.*, 1995, **117**, 1169; (b) E. C. Wilkinson, Y. Dong, Y. Zang, H. Fujii, R. Fraczkiewicz, G. Fraczkiewicz, R. S. Czernuszewicz and L. Que, Jr., *J. Am. Chem. Soc.*, 1998, **120**, 955.

27 L. Shu, J. C. Nesheim, K. Kauffmann, E. Münck, J. Lipscomb and L. Que, Jr., *Science*, 1997, **275**, 515.

28 R. L. Whetten, D. M. Cox, D. J. Trevor and A. Kaldor, *J. Phys. Chem.*, 1985, **89**, 566.

29 (a) A. D. Becke, *J. Chem. Phys.*, 1993, **98**, 5648; (b) *J. Chem. Phys.*, 1992, **97**, 9173; (c) *J. Chem. Phys.*, 1992, **96**, 2155.

30 C. Lee, W. Yang and R. G. Parr, *Phys. Rev. B*, 1988, **37**, 785.

31 C. W. Bauschlicher Jr., *Chem. Phys. Lett.*, 1995, **246**, 40.

32 T. Wagener and G. Frenking, *Inorg. Chem.*, 1998, **37**, 1805.

33 F. A. Cotton and X. Feng, *J. Am. Chem. Soc.*, 1997, **119**, 7514; 1998, **120**, 3387.

34 B. S. Jursic, *Int. J. Quantum Chem.*, 1997, **64**, 255.

35 R. J. Bartlett and G. D. Purvis, *Int. J. Quantum Chem.*, 1978, **14**, 516.

36 G. E. Scuseria and H. F. Schaefer III, *J. Chem. Phys.*, 1989, **90**, 3700.

37 A. D. McLean and G. S. Chandler, *J. Chem. Phys.*, 1980, **72**, 5639.

38 R. Krishnan, J. S. Binkley, R. Seeger and J. A. Pople, *J. Chem. Phys.*, 1980, **72**, 650.

39 A. J. H. Wachters, *J. Chem. Phys.*, 1970, **52**, 1033.

40 P. J. Hay, *J. Chem. Phys.*, 1977, **66**, 4377.

41 K. Raghavachari and G. W. Trucks, *J. Chem. Phys.*, 1989, **91**, 1062.

42 M. J. Frisch, G. W. Trucks, H. B. Schlegel, P. M. W. Gill, B. G. Johnson, M. A. Robb, J. R. Cheesman, T. Keith, G. A. Petersson, J. A. Montgomery, K. Raghavachari, M. A. Al-Laham, V. G. Zakrzewski, J. V. Ortiz, J. B. Foresman, C. Y. Peng, P. Y. Ayala, W. Chen, M. W. Wong, J. L. Andres, E. S. Replogle, R. Gomerts, R. L. Martin, D. J. Fox, J. S. Binkley, D. J. Defrees, J. Baker, J. J. P. Stewart, M. Head-Gordon, C. Gonzalez and J. A. Pople, Gaussian 94 Revision E.2, Gaussian, Inc., Pittsburgh PA, 1995.

43 J. Mestres, Electra, Girona, CAT, 1994.

44 T. Noro, C. Ballard, M. H. Palmer and H. Tatewaki, *J. Chem. Phys.*, 1994, **100**, 452.

45 G. V. Chertihin, A. Citra, L. Andrews and C. W. Bauschlicher, *J. Phys. Chem.*, 1997, **101**, 8793.

46 K. Yoshizawa, T. Ohta, T. Yamabe and R. Hoffmann, *J. Am. Chem. Soc.*, 1997, **119**, 12311.

47 A. Zacarias and M. Castro, *Int. J. Quantum Chem.: Quantum Chem. Symp.*, 1996, **30**, 207.

48 R. F. W. Bader, *Atoms in Molecules: A Quantum Theory*, Clarendon, Oxford, 1990.

Paper 8/03725F